Title

Riverine nitrate source apportionment using dual stable isotopes in a drinking water source watershed of southeast China

Authors

Shang, Xu
Huang, Hong
Mei, Kun
et al.

Publication Date

2020-07-01

DOI

10.1016/j.scitotenv.2020.137975

Peer reviewed

Science of the Total Environment 724 (2020) 137975

Contents lists available at ScienceDirect

Science of the Total Environment

journal homepage: www.elsevier.com/locate/scitotenv

Riverine nitrate source apportionment using dual stable isotopes in a drinking water source watershed of southeast China

Xu Shang [a,c,1], Hong Huang [a,1], Kun Mei [a,c], Fang Xia [a,c], Zheng Chen [a,c], Yue Yang [b], Randy A. Dahlgren [a,c,d], Minghua Zhang [a,c,d], Xiaoliang Ji [a,c,*]

[a] Key Laboratory of Watershed Science and Health of Zhejiang Province, School of Public Health and Management, Wenzhou Medical University, Wenzhou 325035, China
[b] College of Life and Environmental Science, Wenzhou University, Wenzhou 325035, China
[c] Southern Zhejiang Water Research Institute (iWATER), Wenzhou 325035, China
[d] Department of Land, Air and Water Resources, University of California, Davis, CA 95616, USA

HIGHLIGHTS

- Key riverine nitrate contributors were identified in a drinking water source.
- MCMC model quantified the spatial variation of individual nitrate pollution sources.
- Uncertainty, denoting variation strength for source contributions, was quantified.

GRAPHICAL ABSTRACT

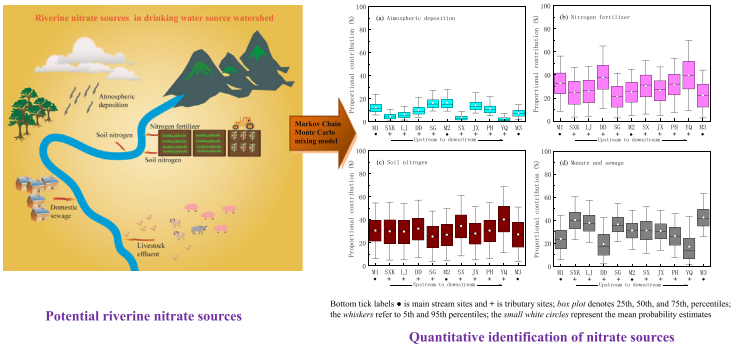

ARTICLE INFO

Article history:
Received 4 December 2019
Received in revised form 9 March 2020
Accepted 14 March 2020
Available online 16 March 2020

Editor: Jay Gan

Keywords:
Riverine nitrate
Drinking water source
Pollution source apportionment
Uncertainty analysis
Stable isotopes
Markov Chain Monte Carlo mixing model

ABSTRACT

It is crucial to quantitatively track riverine nitrate (NO_3^-) sources and transformations in drinking water source watersheds for preventing current and future NO_3^- pollution, and ensuring a safe drinking water supply. This study identified the significant contributors to riverine NO_3^- in Zhaoshandu reservoir watershed of Zhejiang province, southeast China. To achieve this goal, we used hydrochemistry parameters and stable isotopes of NO_3^- ($\delta^{15}N\text{-}NO_3^-$ and $\delta^{18}O\text{-}NO_3^-$) accompanied with a Markov Chain Monte Carlo mixing model to estimate the proportional contributions of riverine NO_3^- inputs from atmospheric deposition (AD), chemical nitrogen fertilizer (NF), soil nitrogen (SN), and manure and sewage (M&S). Results indicated that the main form of riverine nitrogen in this region was NO_3^-, constituting ~60% of the total nitrogen mass on average (total organic nitrogen ~37% & ammonium ~3%). Variations in the isotopic signatures of NO_3^- demonstrated that microbial nitrification of NF, SN and M&S was the primary nitrogen transformation process within the Zhaoshandu reservoir watershed, whereas denitrification was minimal. A classical dual isotope bi-plot incorporating chloride concentrations suggested NF, SN and M&S were the major contributors of NO_3^- to the river. Riverine NO_3^- source apportionment results were further refined using the Markov Chain Monte Carlo mixing model, which revealed that AD, NF, SN and M&S contributed 7.6 ± 4.1%, 22.5 ± 12.8%, 27.4 ± 14.5% and 42.5 ± 11.3% of riverine NO_3^- at the watershed outlet, respectively. Finally, uncertainties associated with NO_3^- source apportionment were quantitatively characterized as: SN > NF > M&S > AD. This work provides a comprehensive approach to distinguish riverine NO_3^- sources

* Corresponding author at: Key Laboratory of Watershed Science and Health of Zhejiang Province, Wenzhou Medical University, Wenzhou 325035, Zhejiang Province, China.
E-mail address: jixiao556677@wmu.edu.cn (X. Ji).
[1] These authors contributed equally to this work.

https://doi.org/10.1016/j.scitotenv.2020.137975

in drinking water source watersheds, which helps guide implementation of management strategies to effectively control NO_3^- contamination and protect drinking water quality.

Summary of the main finding from this works (Capsule): We utilized NO_3^- stable isotope analysis and a Markov Chain Monte Carlo mixing model to quantify riverine nitrate pollution sources in a drinking water source watershed in Zhejiang province, southeast China. Markov Chain Monte Carlo mixing model output showed that NF, SN and M&S were the dominant sources of riverine NO_3^- during the sampling period in Zhaoshandu watershed. Uncertainty analysis characterized the variation strength associated with contributions of individual nitrate sources and indicated the greatest uncertainty for SN, followed by NF, M&S and AD.

1Introduction

The impact of nitrate (NO_3^-) contamination in drinking water sources is a serious global concern, especially in regions where available water resources are scarce. High nitrate concentrations may cause human health risks, such as miscarriage, cancers (e.g., stomach, esophagus, bladder, kidney), and methemoglobinemia ("blue baby" syndrome), as well as several ecological problems, including eutrophication, harmful algal blooms, hypoxia/anoxia and loss of aquatic biodiversity (Burow et al., 2010; Carey et al., 2011; Hord, 2011; Nestler et al., 2011; World Health Organization, 2011).

Riverine NO_3^- concentrations are determined by the interplay between anthropogenic inputs, such as chemical N fertilizer (NF), atmospheric deposition (AD), and manure and sewage (M&S), and natural processes including changes in soil nitrogen (SN) storage, nitrification and denitrification. Riverine NO_3^- source apportionment is one of the most inherently difficult challenges for water resource managers because of the numerous sources of riverine NO_3^- and complex spatial/temporal variations of pollutant inputs and transformations within a given watershed. Notably, preventing future contamination is much more economical and practical compared to its remediation. Therefore, accurately identifying the major contributors/controls on riverine NO_3^- concentrations is essential for developing effective nitrate control and remediation strategies.

More recently, promising environmental stable isotope methods were applied to provide information about NO_3^- sources (e.g., animal waste vs. soil nitrogen) and transformations (e.g., nitrification and denitrification). The theoretical basis for isotopic method results from different NO_3^- sources having distinctive $\delta^{15}N$ and $\delta^{18}O$ isotopic signatures (Biddau et al., 2019). For example, the $\delta^{15}N$ values from AD, SN, NF and M&S range from −13 to +13‰, 0 to +8‰, −6 to +6‰, and +4 to +25‰, respectively (Flipse and Bonner, 1985; Kendall and McDonnell, 1998; Xue et al., 2009). For $\delta^{18}O$ of nitrate, atmospheric deposition and NO_3^- fertilizer are +17 to +25‰ and +25 to +75‰, respectively, while the $\delta^{18}O\text{-}NO_3^-$ values sourced from microbial nitrification of NF, SN and MS are appreciably lower than those of AD and NO_3^- fertilizer, and often vary from −5‰ to +15‰ (Kendall and McDonnell, 1998; Mayer et al., 2001).

Nowadays, several studies reported successful application of the dual stable isotopes of NO_3^- to characterize the sources and processes affecting NO_3^- in water bodies such as Adebowale et al. (2019) and Hu et al. (2019b). Furthermore, to develop quantitative information on NO_3^- source apportionment in water bodies, Xue et al. (2012) introduced a powerful tool known as the Markov Chain Monte Carlo mixing model that was adopted from isotopic analysis of food-webs. They demonstrated that this mixing model was suitable for quantifying contributions of NO_3^- sources to surface waters. Since then, isotopic tracers combined with Markov Chain Monte Carlo mixing models were extensively utilized to obtain the proportional contributions of NO_3^- from independent sources. For instance, Li et al. (2019) employed the Markov Chain Monte Carlo mixing model to track NO_3^- sources in the Xijiang River (China). Their results revealed that SN and NF were the dominant (72–73%) NO_3^- sources in the wet season, whereas approximately 58% of NO_3^- originated from anthropogenic inputs (M&S and NF) in the dry season. Most previous studies examined highly polluted water systems. In contrast, few studies investigated sources of riverine NO_3^- in drinking water source watersheds for the purpose of protecting the vital water resources from further pollution (Zhang et al., 2018).

Considering spatio-temporal variations of isotopic composition, isotopic fractionation, and multiple NO_3^- sources, NO_3^- source apportionment methods incorporate inherent uncertainties. Parnell et al. (2010) and von Toussaint (2011) specified that point estimates (e.g., posterior mean value) should be used with caution for evaluating proportional contributions since they tend to lose important information concerning uncertainty. Liu et al. (2013) highlighted the need for uncertainty analysis when calculating proportional contributions of NO_3^- sources due to the broad range of isotopic signatures for various NO_3^- sources. According to statistical and probability theory, the Markov Chain Monte Carlo method is capable of providing a complete posterior probability distribution, in contrast to unique values, for the proportional contribution of each NO_3^- pollution source. This provides a distinct advantage in using the Markov Chain Monte Carlo mixing model with stable isotopes by enabling assessment of the uncertainty associated with the NO_3^- source apportionment results. The lack of uncertainty analysis in previous studies greatly limits the interpretation of quantitative apportionment for practical applications of water resource management.

In view of the above considerations, the objectives of this study were to: (1) apportion the sources of riverine NO_3^- in a typical drinking water supply watershed of southeast China through the joint application of dual-isotopic analysis and Markov Chain Monte Carlo mixing models; and (2) investigate the uncertainty associated with Markov Chain Monte Carlo mixing model estimates. Results of this study enhance our understanding of NO_3^- sources, and the fate and transport of NO_3^- at the large watershed scale. Further, the results provide scientific information for developing and implementing NO_3^- pollution control plans to ensure a sustainable clean water supply.

2Materials and methods

2.1Study area

The Shanxi drinking water source region (27°36′–27°50′ N, 119°47′–120°15′ E) is located in the uplands of the Feiyun River in Zhejiang province of southeast China and occupies a total drainage area of ~2300 km^2 (Huang et al., 2018) (Fig. 1). The system consists of upstream (Shanxi = 1.8×10^9 m^3) and downstream (Zhaoshandu = 3.4×10^7 m^3) reservoirs that provide drinking and municipal water for the city of Wenzhou (~9.2 million population). Climate in the study area is subtropical monsoon with cold, dry winters and hot, rainy summers. Average annual rainfall is ~1880 mm with approximately 75% of the precipitation occurring during April–September (Huang et al., 2017). Annual average temperature, sunshine hours, and relative humidity are 19.60 °C, 1887 h and 83%, respectively. Primary land-use categories in the watershed are forest (75%) and agricultural land (15%) along with <5% residential land. Typical agricultural crops in the watershed included rice, sweet potato, pea, soybeans, tea, melons, oranges, bayberry and vegetables. Approximately 0.55 million

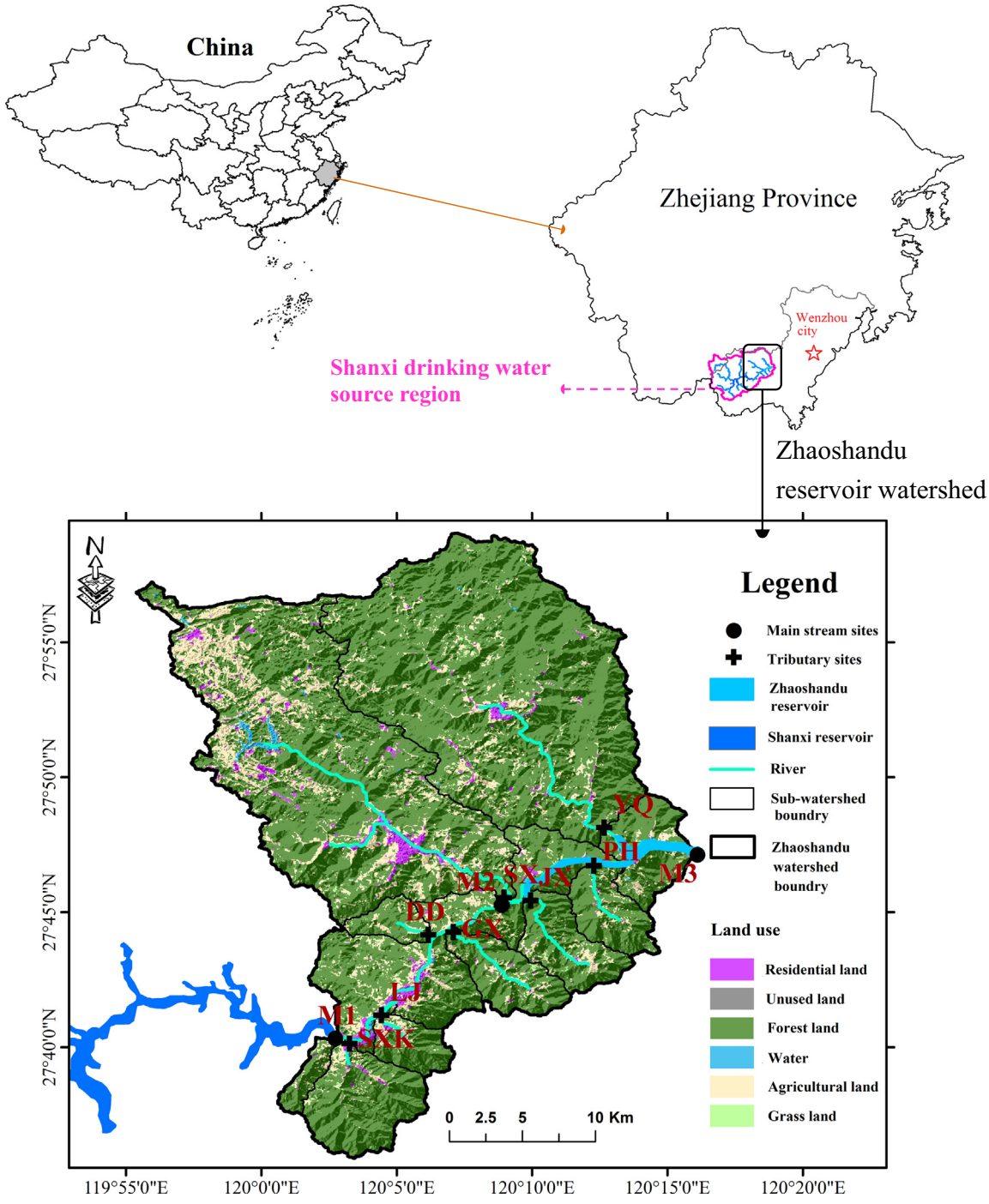

Fig. 1. Location of the Zhaoshandu reservoir watershed and sampling sites.

people live within the watershed. Current livestock and poultry population consists of 2803 pigs, 1078 cows, 5562 sheep, 59,800 rabbits, 60,600 chickens, and 49,900 ducks. Red soils (Oxisols/Ultisols in Soil Taxonomy) are the dominant soil type in the watershed. Terrain within the watershed is dominated by mountains and hills with considerable topographic relief (average relief = 31.5%); elevations range from 9 to 1663 m, with an average of 573 m (Huang et al., 2017). The hydrogeomorphology of the upland river system consists of sandstone aquifers.

This study focused on water quality released from Zhaoshandu reservoir as it represents an integrator site for the entire upstream watershed and it is the diversion point for the source water utilized for municipal use. The tandem reservoirs consist of a multi-annual regulating reservoir (Shanxi reservoir — mean water residence time = ~1 yr) with a downstream water diversion reservoir (Zhaoshandu reservoir — mean water residence time = ~5 days) located ~30 km downstream (Huang et al., 2017). Given this configuration, the reservoir releases represent a time and space integrated sample for the entire watershed area. To better understand the spatial distribution of nitrate sources, we examined water released from the upstream Shanxi Reservoir and several tributary inputs between Shanxi and Zhaoshandu reservoirs. Approximately 70% of the water released from the downstream Zhaoshandu reservoir originates from Shanxi reservoir releases. Therefore, the tributary inputs between Shanxi and Zhaoshandu reservoirs contribute only a small water volume compared to Shanxi reservoir. Point source nutrient pollution was largely eliminated within

the watershed area as polluting industries were forced to close or move outside the water source conservation area by regulatory authorities to protect drinking water sources in 2012. Thus, the primary sources of NO_3^- in the watershed originate from nonpoint sources associated with atmospheric deposition (AD), N fertilizer (NF), soil nitrogen (SN), and manure and sewage (M&S).

2.2Water sampling and laboratory analysis

Surface water sampling was conducted under stormflow condition in June 2019 when eutrophication potential was most pronounced. We collected water samples from 11 sampling sites using a hydrophore sampler from a 30-cm depth in the center of a well-mixed stream segment between 10:00 and 14:00 within a single day. Eight sites were located in tributary streams (Yuquan (YQ), Jiuxi (JX), Sixi (SX), Shuanggui (SG), Dudu (DD), Lijing (LJ), Shanxikeng (SXK), and Pinghe (PH)), and three sites were located along the mainstem of the Feiyun River from upstream (M1) to midstream (M2) and downstream (M3) (Fig. 1). Dissolved oxygen (DO) was determined in situ using a multi-parameter water-quality sonde (EXO2, YSI, USA). We collected ~500 mL of water at each site in a precleaned, high-density polyethylene bottle. Samples were stored on ice and transported to the laboratory for quantification of total nitrogen (TN), ammonium (NH_4^+), nitrite (NO_2^-), nitrate (NO_3^-), total organic nitrogen (TON), total phosphorus (TP), phosphate (PO_4^{3-}), total organic carbon (TOC), chloride (Cl^-), δ^{15}N-NO_3^- and δ^{18}O-NO_3^-. TN, TP and TOC were determined on non-filtered samples while dissolved constituents were determined on samples filtered through a 0.45 μm Millipore nitrocellulose membrane. TN and TP were determined as NO_3^- and PO_4^{3-}, respectively, following persulfate oxidation. Concentrations of NO_3^-, NH_4^+, NO_2^-, and PO_4^{3-} were determined using a continuous flow analyzer with a limit of detection of ~0.003 mg/L (AA3, Seal, Germany). Herein, we estimated TON as: TON = TN – NH_4^+ – NO_3^- – NO_2^- (Sarkkola et al., 2009; Li et al., 2017). TOC and Cl^- were measured using a TOC analyzer (limit of detection ~ 0.1 mg C/L; TOC-L, Shimadzu, Japan) and ion chromatography system (limit of detection ~0.001 mg/L; Compact IC plus 882, Metrohm, Switzerland), respectively.

For dual δ^{15}N-NO_3^- and δ^{18}O-NO_3 isotope analysis, 20 mL of filtered sample was transported on ice to the Environmental Stable Isotope Lab at the Chinese Academy of Agricultural Sciences (Beijing, China). The δ^{15}N-NO_3^- and δ^{18}O-NO_3^- values were obtained using the denitrifier method to convert NO_3^- to gaseous nitrous oxide by *Pseudomonas aureofaciens* for detection using a continuous-flow isotope ratio mass spectrometer (IRAM, Isoprime100, Cheadle, UK). Stable isotope ratios are expressed in parts per thousand (‰) relative to atmospheric N_2 and Vienna Standard Mean Ocean water for δ^{15}N-NO_3^- and δ^{18}O-NO_3^-, respectively (Kendall et al., 2007). Sample analysis had an average precision of ±0.20‰ for δ^{15}N-NO_3^- and ± 0.50‰ for δ^{18}O-NO_3^-. Additional details regarding the denitrifier method can be found in Ji et al. (2017).

2.3Markov Chain Monte Carlo mixing model

We employed the Markov Chain Monte Carlo mixing model to quantify the proportional contribution of each potential source to the mixture of riverine NO_3^- in surface waters. The linear mass-balance mixing model can be solved using the Markov Chain Monte Carlo method with a Bayesian framework based on the assumption that the proportional source contribution follows a Dirichlet distribution (Parnell et al., 2010). The Markov Chain Monte Carlo technique uses random sampling from both prior knowledge of unknown parameters (i.e., proportional contributions of different sources) and probability distributions for each input variable (i.e., NO_3^- source; isotope fractionation factor). Equations for the system model were:

}\fleqno \rm \kern-10pt(1)

whereX_{ij}representstheobservedisotopecompositionjofthemixture(watersample)i; S

Based on field investigations and previous research findings (Dong et al., 2016; Huang et al., 2017), we assumed that the riverine NO_3^- content in Zhaoshandu watershed was primarily attributable to inputs from AD, NF, SN and M&S. Isotopic signatures for these designated sources were obtained from the nearby Changle River watershed (~180 km) (Ji et al., 2017). The δ^{18}O-NO_3^- value for NF was amended based on the δ^{18}O signature of atmospheric O_2 and ambient water from Fuzhou station (~190 km). Table 1 summarizes the mean values and standard errors for each of the NO_3^- sources. The model operational parameters were set as: run iterations = 500,000; burn-in = 50,000; sample interval = 15; and iteration maintainer = 30,000.

Uncertainty index

The uncertainty index (UI_{90}) was defined by Ji et al. (2017) for characterizing uncertainty based on the posterior distribution and represents the difference of proportional contribution between the minimum and maximum values of the rapidly increasing segment (90% cumulative probability) divided by a given certain probability (90%) (Fig. S1, Supplementary material). UI_{90} denotes the uncertainty strength under a high probability condition (90%) and thereby eliminates the effect of extreme values having a small probability (10%). Thereby, UI_{90} was calculated to delineate the degree of uncertainty associated with apportionment results.

Results and discussion

Water quality characteristics

A summary of water quality variables measured at the 11 sampling sites in the Zhaoshandu reservoir watershed during the investigative period is provided in Table 2. Water quality values for each independent site and the corresponding water quality standards for surface water in China (GB3838-2002) (State Environment Protection Bureau of China, 2002) are listed and described in Tables S1 and S2 (Supplementary material), respectively.

The coefficient of variation for the water quality variables ranged from 14.6 to 116.9%, implying considerable spatial variability among sampling sites (Yang et al., 2013b) (Table 2). DO concentrations varied from 4.50 to 7.30 mg/L, with most of the samples classified as meeting the type III water quality standard (≥5 mg/L). The higher levels of DO signified that the surface waters of Zhaoshandu watershed are not favorable for denitrification, but some denitrification may occur within anoxic sediments within the system (Rivett et al., 2008).

Excessive nitrogen derived from non-point source pollution is considered the most serious pollutant in Zhaoshandu reservoir (Xiao

Table 1
Specific δ^{15}N and δ^{18}O values of potential NO_3^- sources.

Source	*n*	δ^{15}N		δ^{18}O	
		Mean	SD	Mean	SD
AD	6	−1.49	1.75	58.18	14.22
NF	4	−0.53	0.22	4.14[a]	1.89[a]
SN	6	2.18	2.59	0.63	2.01
M&S	7	10.49	4.53	3.45	2.63

[a] The value of δ^{18}O-NO_3^- in chemical fertilizer is calculated based on the measured δ^{18}O values of atmospheric O_2 and ambient water at nearby Fuzhou station.

Table 2
Descriptive statistics of water quality variables (mg/L).

Parameters	*N*	Mean	SD	CV (%)	Minimum	Maximum
DO	11	5.91	0.86	14.6	4.50	7.30
TN	11	1.52	0.70	46.3	0.85	3.04
NH_4^+-N	11	0.04	0.05	102.4	<0.01	0.14
NO_2^--N	11	0.02	0.02	116.3	<0.01	0.08
NO_3^--N	11	0.90	0.42	47.2	0.46	1.84
TON	11	0.56	0.28	49.59	0.04	0.98
TP	11	0.03	0.03	90.9	0.01	0.12
PO_4^{3-}-P	11	0.02	0.02	116.9	<0.01	0.09
Cl^-	11	1.96	0.49	25.1	1.31	2.78
TOC	11	2.02	0.89	44.1	0.96	3.97

N number of samples, SD standard deviation, CV coefficient of variation.

et al., 2011). TN concentrations ranged from 0.85 to 3.04 mg/L, with an average of 1.52 mg/L. In terms of water quality standards, 100% and ~65% of the samples did not meet the desired type II water quality standard of 0.50 mg/L (acceptable as first-grade protection zone for centralized drinking water source) and type III water quality standard of 1.00 mg/L (lower threshold for drinking water), respectively. The average NH_4^+ and NO_2^- concentrations were 0.04 mg/L (range ≤ 0.01–0.14 mg/L) and 0.02 mg/L (range ≤ 0.01–0.08 mg/L), respectively, and all samples complied with type I water quality standards for NH_4^+ (0.15 mg/L). Mean NO_3^- concentration was 0.90 mg/L (range = 0.46–1.84 mg/L) and was the dominant form of N (~60% of TN) in the watershed. While the NO_3^- concentrations were far below the 10 mg NO_3^-/L limit for drinking water set by the World Health Organization, the high NO_3^- may contribute to harmful algal blooms that render the water unsuitable as a drinking water source, as well as ecological degradation. TON concentrations varied from 0.04 to 0.98 mg/L with an average value of 0.56 mg/L that represented ~37% of TN making it a much higher contributor of nitrogen than NH_4^+ and NO_2^-, but lower than NO_3^-.

Average TP concentration was 0.03 mg/L (range = 0.01–0.12 mg/L) and most sites complied with the type II water quality standard (0.1 mg/L for river and 0.025 mg/L for reservoir). PO_4^{3-} concentrations ranged from <0.01 to 0.09 mg/L. Concentrations of Cl^- ranged between 1.31 and 2.78 mg/L and TOC between 0.96 and 3.97 mg/L. These results demonstrate that the major surface water issue in the Zhaoshandu watershed was elevated NO_3^- concentrations. Consequently, identifying the riverine NO_3^- sources is a priority for water managers to protect water quality in the Zhaoshandu reservoir system.

Isotopic composition of NO_3^-

The δ^{15}N-NO_3^- and δ^{18}O-NO_3^- values for water samples in the Zhaoshandu watershed ranged between 0.93 and 6.41‰ and 2.74–10.92‰, respectively (Fig. 2a). Dual stable isotopic (δ^{15}N-NO_3^- and δ^{18}O-NO_3^-) signatures can provide meaningful insights into nitrogen transformation processes (i.e., nitrification and denitrification) controlling NO_3^- content within watersheds (Li et al., 2019; Yang and Toor, 2016).

As for nitrification, the δ^{18}O-NO_3^- composition of the newly produced NO_3^- depends on the δ^{18}O values of ambient water and air (Mayer et al., 2001; Wassenaar, 1995). In theory, nitrifying bacteria utilize two oxygen atoms from the surrounding water and one oxygen atom from atmospheric oxygen for oxidizing NH_4^+ to NO_3^- (Kendall and McDonnell, 1998). According to the δ^{18}O of 23.50‰ for atmospheric O_2 and −14.16‰ to −0.92‰ in ambient water collected from a nearby station of the International Atomic Energy Association station at Fuzhou (~190 km), microbially-produced δ^{18}O-NO_3^- values were estimated to range within −1.61‰–7.22‰. It has, however, been documented that microbially-produced δ^{18}O-NO_3^- can exceed this calculated theoretical maximum by up to 5‰ (Kendall, 1998; Mayer et al., 2001; Xue et al., 2009). Samples from Zhaoshandu watershed had δ^{18}O-NO_3^- values in the range of −1.61‰–12.22‰. This local theoretical range provided clues about the role of microbial nitrification in producing NO_3^- (Li et al., 2010; Yang et al., 2013a; Wexler et al., 2014). Namely, the isotopic compositions of δ^{18}O-NO_3^- for all samples (2.74–10.92‰) fell within the expected domain for a microbial nitrification source (−1.61–12.22‰). Furthermore, nitrogen in SN, NF, and M&S is mostly in reduced forms and thereby riverine NO_3^- derived from these sources will undergo microbial nitrification (Kendall and McDonnell, 1998; Yang et al., 2013a). Consequently, we posit that the riverine NO_3^- originated largely from nitrification of NF, SN and M&S sources.

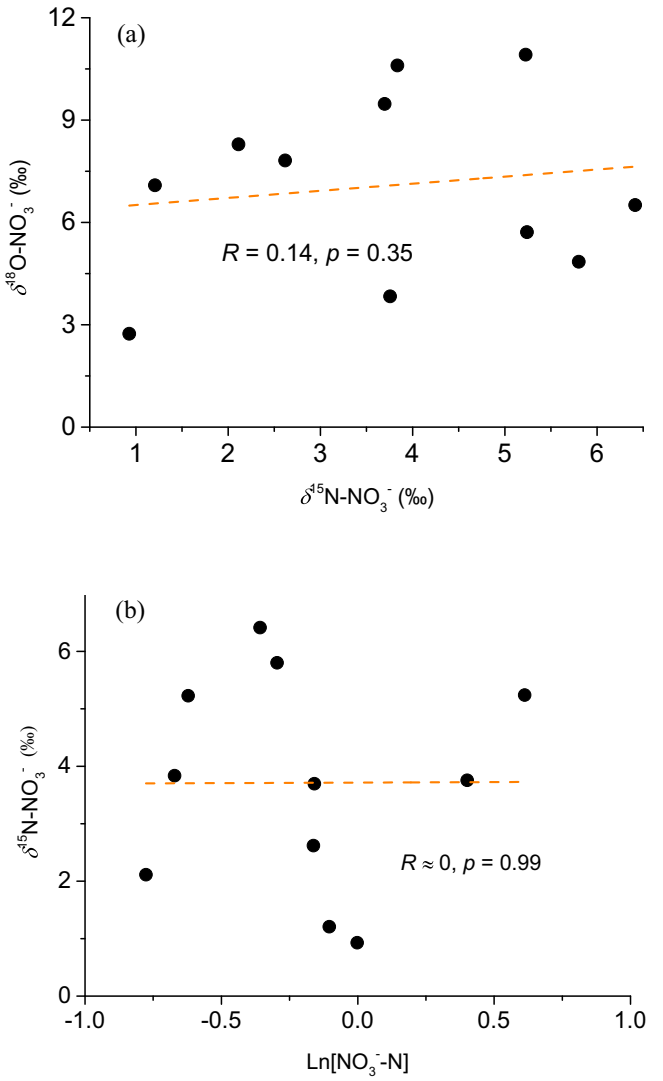

Fig. 2. (a) Relationship between δ^{15}N-NO_3^- and δ^{18}O-NO_3^- values, and (b) relationship between δ^{15}N-NO_3^- and NO_3^--N concentrations in the Zhaoshandu reservoir watershed.

Denitrification results in a progressive decrease in NO_3^- concentrations with a corresponding increase in both δ^{15}N-NO_3^- and δ^{18}O-NO_3^- in the residual NO_3^- fraction. The denitrification enrichment ratio for δ^{18}O-NO_3^-:δ^{15}N-NO_3^- generally ranges within 0.4–0.7 in the field and up to 1.0 in the laboratory (Aravena and Robertson, 1998; Granger et al., 2008; Liu et al., 2006; Mariotti et al., 1981). As illustrated in Fig. 2a, a significant positive linear relationship was not found between δ^{18}O-NO_3^- and δ^{15}N-NO_3^-. Additionally, no significant negative relationship existed between NO_3^- concentrations and δ^{15}N-NO_3^- (Fig. 2b). Therefore, we conclude that denitrification was not a dominant nitrogen transformation process in the Zhaoshandu watershed during the sampling period. The generally aerobic conditions (DO > 2 mg/L) within the surface waters inhibit denitrification (an anaerobic process); however, some denitrification may occur in the anoxic subsurface soils/sediments and groundwater within the aquatic system.

Qualitative identification of NO_3^- sources

With the aim of acquiring qualitative information about the dominant sources affecting NO_3^- concentrations in the river system, we utilized a classical dual isotope bi-plot approach. The δ^{15}N-NO_3^- vs. δ^{18}O-NO_3^- of samples was plotted along with isotope envelopes characterizing potential NO_3^- sources that could influence surface water. Our sampling points for δ^{15}N-NO_3^- vs. δ^{18}O-NO_3^- did not fall into the "AD" source window, indicating little or no riverine NO_3^- contribution directly from AD (Fig. 3). However, it is important to consider that most atmospheric nitrate inputs to receiving waters undergo some processing within the watershed thereby obscuring the identity of the AD source (Sebestyen et al., 2019). In contrast, six points fall in the NF-SN-M&S overlap zone, four points lie within the NF-SN overlap zone, and the remaining one point falls in the SN-M&S overlap zone. This assessment infers that NF, SN and M&S are the likely primary contributors of NO_3^- in the Zhaoshandu watershed.

Elevated riverine Cl^- concentrations are derived from various anthropogenic origins (e.g., human/livestock waste), and thereby Cl^- is often an effective indicator of mixing between different pollutant sources. Given that Cl^- acts as a conservative tracer, it can often serve as an indicator of different pollutant sources (Widory et al., 2004; Xi et al., 2015). For example, NF is generally characterized as having high NO_3^- contents with low Cl^- contents, while M&S has a high Cl^- content resulting in a low NO_3^-/Cl^- molar ratio (Liu et al., 2006). In addition, as a natural source, SN has a low Cl^- content along with a low NO_3^-/Cl^- ratio. Therefore, investigation of the NO_3^-/Cl^- molar ratio versus Cl^- molar concentration often provides additional information for NO_3^- source identification. Corresponding data from the study site indicated moderate levels of Cl^- and NO_3^-/Cl^- molar ratios indicating that riverine NO_3^- was affected by anthropogenic inputs, such as M&S (Fig. 4).

Quantitative tracking of NO_3^- sources

Although the dual isotope bi-plot approach applied to the data set provided qualitative results about the sources of NO_3^-, it fails to give a quantitative assessment regarding the proportional contribution from each source type. Ideally, a quantitative assessment is necessary for helping decision makers and stakeholders develop appropriate strategies to control nitrate pollution at the watershed scale. Here, we employed a Markov Chain Monte Carlo mixing model to quantify NO_3^- source apportionment. Based on our initial analyses, denitrification

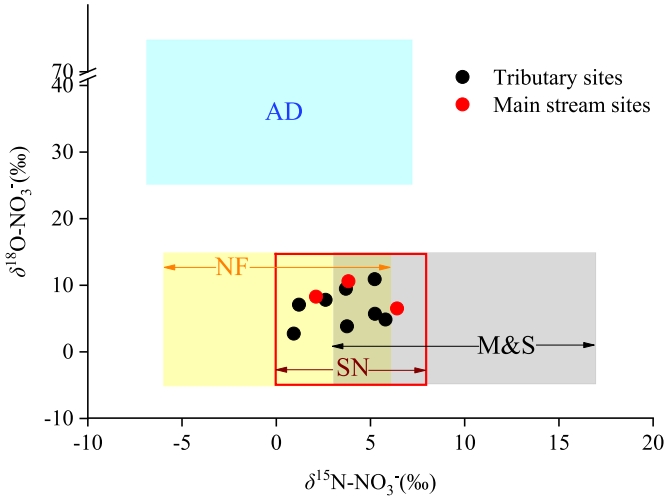

Fig. 3. Isotopic signatures of δ^{15}N-NO_3^- and δ^{18}O-NO_3^- for river water samples and potential NO_3^- sources in the Zhaoshandu reservoir watershed. The isotopic ranges of the four suspected dominant sources were adapted from Nestler et al. (2011) with updated values from Xu et al. (2014).

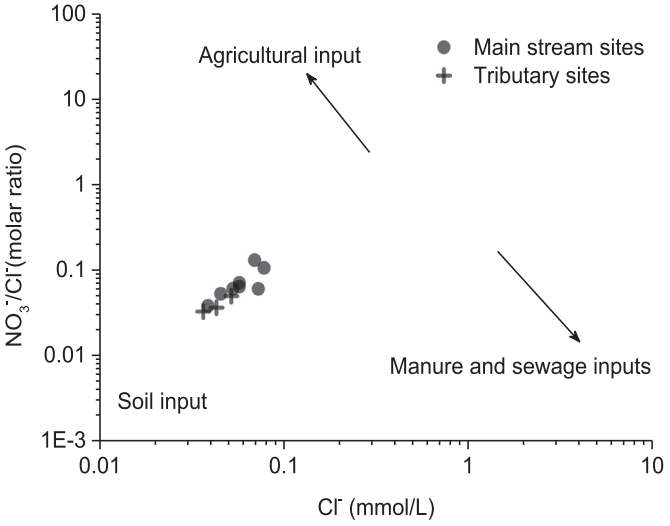

Fig. 4. NO_3^-/Cl^- molar ratio with Cl^- molar concentration in the Zhaoshandu reservoir watershed.

was assumed to be negligible in the Zhaoshandu system and was therefore not considered in the model.

Fig. 5 illustrates the proportional contributions for the four potential NO_3^- sources estimated by the Markov Chain Monte Carlo mixing model. High variability was evident for the proportional contribution of each potential NO_3^- source among sampling sites because of site-specific nitrogen emissions, along with differences in transport and fate dynamics of NO_3^- during delivery from each source to the receiving waters. From the mean probability estimate, AD was the lowest source contribution (2.8 ± 3.2–16.5 ± 5.6%) among all sites. The NF source exhibited a contribution of 21.5 ± 11.8–39.7 ± 17.7%, along with a similar contribution from SN (25.5 ± 13.3–40.3 ± 16.8%). The highest estimates (>30%) for NF and SN were observed at five sampling sites (YQ, SX, DD, PH and M1). M&S contributions fell a range of 17.1 ± 13.3–42.5 ± 11.3% with the highest value (42.5 ± 11.3%) at Zhaoshandu reservoir outlet (M3). Markov Chain Monte Carlo mixing model outputs were consistent with the general results of dual isotope bi-plots as they both indicated that NF, SN and M&S were dominant sources of riverine NO_3^- during the sampling period. However, the Markov Chain Monte Carlo mixing model provided more precise information on the predominant NO_3^- sources, as well as other potential sources.

As for the Zhaoshandu reservoir outlet site (M3 — the integrator site for the entire watershed), riverine NO_3^- concentrations followed M&S (42.5 ± 11.3%) > SN (27.4 ± 14.5%) > NF (22.5 ± 12.8%) > AD (7.6 ± 4.1%). Nowadays, pollution from livestock within the Shanxi drinking water source region (upper reservoir) is highly regulated. Following a strict ban on large-scale livestock and poultry breeding farms in 2012, the amount of livestock decreased remarkably from 182,602 to 15,163 pig-equivalents during the 2010–2017 period. Nevertheless, there are many villages located near the river having poor municipal infrastructure that leads to untreated domestic wastewater being directly discharged into the river system. This untreated or incompletely treated domestic sewage is believed to be the primary component of M&S pollution at this time. This finding was further supported by the progressive increase in M&S contribution together with NO_3^- concentrations from M1 → M2 → M3 (Figs. 5 and S2). Annual NF application rates in this region are ~518 kg N/ha, which is ~1.7 times the national average (300 kg N/ha). There was an estimated 6.01 × 10^6 kg (=518 kg N/ha/yr × 77,400 ha × 15% agricultural land area) of nitrogen fertilizer applied in the watershed annually. Liao (2015) estimated the amount of nitrogen deposited from the atmosphere to be ~34 kg/ha/yr, indicating that AD inputs were approximately 2.63 × 10^6 kg annually (=34 kg/ha/yr × 77,400 ha), which was ~50% of NF inputs. However, unprocessed

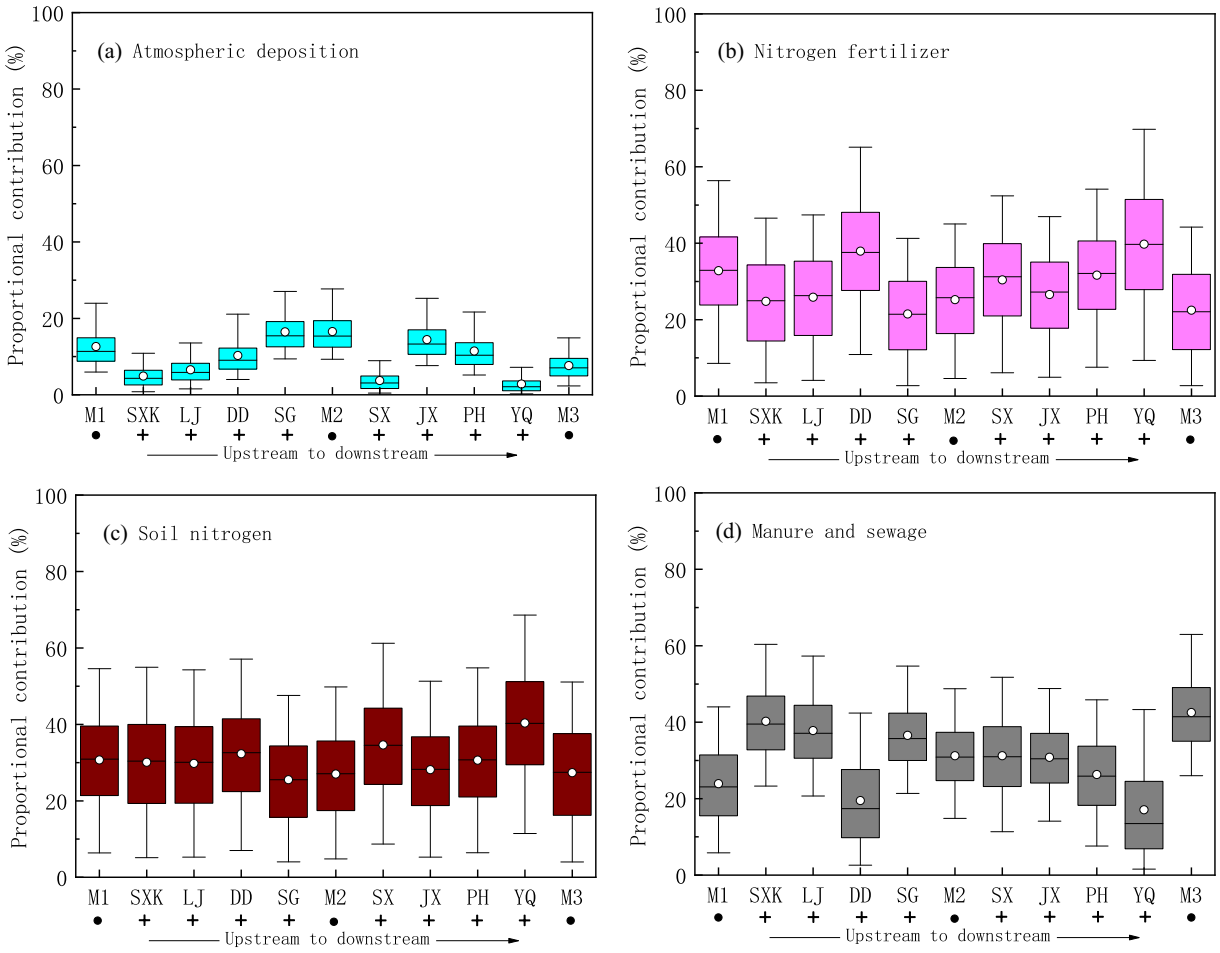

Fig. 5. Proportional contributions of four potential NO_3^- sources at different sampling sites according to the Markov Chain Monte Carlo mixing model. Bottom tick labels: ● is main stream sites and + is tributary sites; *box plot* denotes 25th, 50th, and 75th, percentiles; the *whiskers* refer to 5th and 95th percentiles; the *small white circles* represent the mean probability estimates.

atmospheric nitrate only accounted for 7% of the total nitrate estimated in the reservoir release waters. Two main phenomena may contribute to this discrepancy. First, much of the nitrate from atmospheric deposition infiltrates into soils and may accumulate in shallow subsurface water or groundwater (i.e., transient storage). Second, most atmospherically-deposited nitrate is taken up by plants/microorganisms within the watershed and/or undergoes significant biological processing (e.g., denitrification) before transport to receiving waters via surface runoff or baseflow. In China, nitrogen utilization efficiency is only ~35% (Yu and Shi, 2015) resulting in large amounts of unutilized NF remaining in the soil system as a legacy nitrogen source (Chen et al., 2018). This NF may be lost to rivers or transformed to SN via soil microbial nitrogen-cycling processes (e.g., assimilation) and soil colloid adsorption. Thus, NF and SN contributed appreciable NO_3^- loads to Zhaoshandu watershed. As illustrated by this watershed analysis, the Markov Chain Monte Carlo mixing model results provide a more precise NO_3^- source apportionment for local water resource protection agencies to develop more site-specific and scientific-based riverine NO_3^- control strategies that directly target the major NO_3^- sources.

Management strategies

According to the NO_3^- source contributions determined above, effective methods for attenuating riverine NO_3^- pollution in the Zhaoshandu watershed should consider: (1) developing/improving waste water treatment plants and expanding sewage pipeline systems, combined with small septic systems or constructed wetlands to minimize domestic sewage discharge without proper treatment; (2) applying fertilizer/manure nitrogen amounts in accordance with crop demands and soil nutrient availability during different plant growth stages; (3) using controlled release and stabilized fertilizers instead of conventional fertilizers to increase the fertilizer utilization rate and decrease NO_3^- leaching; and (4) adopting widespread recycling of farmland drainage for paddy irrigation to enhance nitrogen removal. Additionally, best management practices (i.e., buffer strips, riparian plantings and constructed wetland) should be implemented to reduce runoff from SN, NF and manure applications to further enhance riverine NO_3^- pollution mitigation (National Research Council, 2001; Haas et al., 2017; Zak et al., 2018).

Uncertainty analysis

Uncertainty is a crucial issue to address in quantitative identification of riverine NO_3^- pollution sources. The posterior probability estimates for individual source contributions obtained by the Markov Chain Monte Carlo mixing model had relatively wide ranges, which reflect large uncertainty in modeled apportionment results (Fig. 6). Most previous studies provided deterministic evaluations of source contributions that only reported mean probability estimate, while the uncertainties associated with the mean probability estimate values were not specified (Ding et al., 2014; Li et al., 2019; Lu et al., 2015).

Markov Chain Monte Carlo mixing models have the ability to provide both point (e.g., mean probability estimate, median value) and interval (e.g., 95% credible interval) contribution estimates. Taking NF at

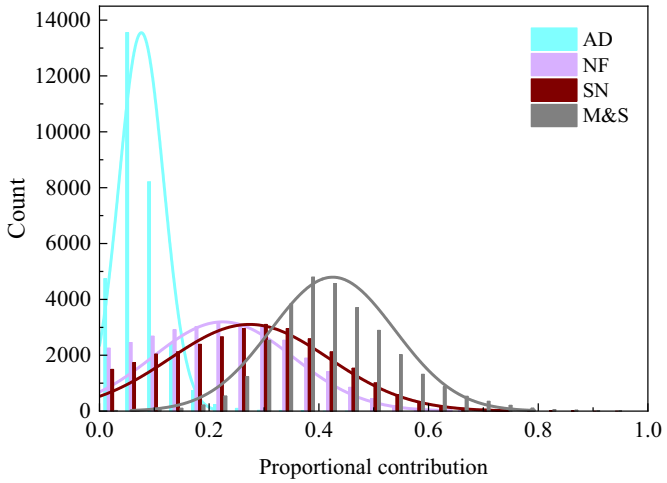

Fig. 6. Histograms (bar) and probability densities (line) of the proportional contribution for four potential NO_3^- sources estimated by the Markov Chain Monte Carlo mixing model using the watershed outlet sampling site (M3) as an example.

the M3 site (Zhaoshandu reservoir outlet) as an example (Fig. 7), the Markov Chain Monte Carlo model determined a point estimate of 22.5% (mean probability estimate), but also that there were 50% and 5% probabilities that the contribution was >22.1% (median value) and 42.2%, respectively, and 95% of the predicted contribution values ranged within 1.4–47.8% (95% confidence interval).

Table 3 displays the results of the UI_{90} calculated to compare the uncertainty levels for the proportional contribution of each source. The UI_{90} values for AD fell into a range of 0.08–0.20. These small values demonstrate that the contribution of AD was relatively stable. The largest uncertainty was associated with the SN contribution as reflected by the high UI_{90} values (0.48–0.63). Similarly, large uncertainties were exhibited in the UI_{90} values for NF (0.43–0.67) and M&S (0.37–0.46). These values were lower than those for SN, but much higher than those of AD. The average UI_{90} values for each pollution source followed: SN (0.54) > NF (0.51) > M&S (0.42) > AD (0.16). This indicates that the uncertainty of different sources exhibited differential variability, largely

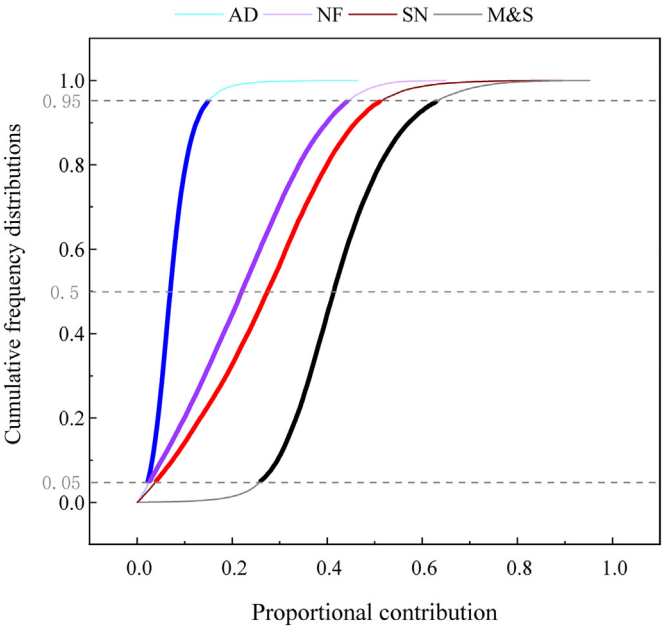

Fig. 7. Cumulative probability distributions of the proportional contributions from four potential NO_3^- sources for the watershed outlet sampling site (M3).

due to the inherent uncertainty associated with source isotopic composition.

To reduce uncertainties associated with NO_3^- apportionment results, specific isotopic measurements of local atmospheric deposition, fertilizer, soil nitrogen, and manure & sewage are necessary for locations throughout the watershed. These data should provide a narrower and more accurate range of local nitrate sources. Additionally, we acknowledge that a single sampling event hinders the full interpretation of nitrate source dynamics and transformations, even at watershed temporal/spatial integrator sites such as the reservoirs used in this study. Therefore, dual isotope records collected for long periods (e.g., annual & seasonal scales), under different flow conditions (low, medium and high flows), as well as high frequency sampling during storm events, are strongly warranted.

A more rigorous temporal sampling design would enhance insights to processes affecting temporal variability of different nitrate sources, and further address possible changes in NO_3^- sources associated with contrasting hydrologic flowpaths (e.g., groundwater, soil interflow, surface runoff). For example, previous research demonstrated that NO_3^- can be transformed en route to rivers from subsurface soil and groundwater flowpaths (Hu et al., 2019a; Miller et al., 2016; Schilling and Zhang, 2004). Given that the potential for oxygen deficiency in subsurface soil and groundwater exists, microbial denitrification may alter the original isotopic composition of NO_3^-. Therefore, fractionation associated with denitrification requires further investigation when interpreting changes in isotopic composition between the initial NO_3^- source and residual NO_3^- fraction discharged into surface waters.

The Shanxi drinking water source watershed considered in this study is one of the largest centralized water sources in the Zhejiang province of China. It is capable of supplying 1.34 billion m^3/yr of potable water for >5 million inhabitants. Here, we collected information from two large reservoirs that provide both a temporal (~1 yr) and spatial (entire watershed area) integration of water inputs. Such samples are much less susceptible to temporal/spatial variability of unregulated watersheds where large changes in water quality occur on storm event and seasonal time scales. Thus, the use of temporal/spatial integrator sites provides an effective approach to reduce uncertainty at the watershed scale.

Conclusions

This study demonstrated that NO_3^- was the predominant component contributing to water quality impairment in the Zhaoshandu reservoir watershed of southeast China. Variations in $\delta^{15}N\text{-}NO_3^-$ and $\delta^{18}O\text{-}NO_3^-$ isotopic signatures indicated that riverine NO_3^- originated largely from the nitrification of NF, SN and M&S sources. By contrast, there was no evidence for microbial denitrification, which was consistent with the generally aerobic conditions associated with the surface water system. A classical dual isotope bi-plot coupled with Cl^- concentrations provided support for the riverine NO_3^- consisting of a mixture of NF, SN and M&S inputs. A Markov Chain Monte Carlo mixing model quantified source apportionment and found that the proportional contributions of NO_3^- sources were highly variable among sampling sites. At the watershed outlet, M&S contributed the most NO_3^- (42.5 ± 11.3%) to the river system, followed by SN (27.4 ± 14.5%), NF (22.5 ± 12.5%), and AD (7.6 ± 4.1%). Finally, an uncertainty analysis associated with the apportionment results quantitatively characterized an uncertainty trend for the individual sources of SN > NF > M&S > AD. Outcomes of this study provided specific recommendations for reducing the uncertainty of the dual NO_3^- isotopic approach ($\delta^{15}N\text{-}NO_3^-$ and $\delta^{18}O\text{-}NO_3^-$) for source apportionment, and demonstrated the efficacy of the method for providing quantitative data for developing beneficial management practices to protect drinking water sources from NO_3^- impairments at the watershed scale.

Table 3
Uncertainty index of each source at different sampling sites.

Source	YQ	JX	SX	SG	DD	LJ	SXK	PH	M1	M2	M3	Average
AD	0.08	0.20	0.09	0.20	0.19	0.13	0.11	0.18	0.20	0.20	0.14	**0.16**
NF	0.67	0.47	0.51	0.43	0.60	0.48	0.48	0.52	0.53	0.45	0.46	**0.51**
SN	0.63	0.51	0.58	0.48	0.56	0.54	0.55	0.54	0.54	0.50	0.52	**0.54**
M&S	0.46	0.39	0.45	0.37	0.44	0.41	0.41	0.42	0.42	0.38	0.41	**0.42**

Declaration of competing interests

The authors declare that they have no known competing financial interests or personal relationships that could have appeared to influence the work reported in this paper.

CRediT authorship contribution statement

Xu Shang: Conceptualization, Methodology, Formal analysis.**Hong Huang:**Conceptualization, Methodology.**Kun Mei:**Investigation.**Fang Xia:**Investigation.**Zheng Chen:**Investigation.**Yue Yang:**Investigation. **Randy A. Dahlgren:**Formal analysis, Writing - original draft, Writing - review & editing.**Minghua Zhang:**Formal analysis.**Xiaoliang Ji:**Conceptualization, Methodology, Formal analysis, Writing - original draft, Writing - review & editing.

Acknowledgements

This work was funded by the National Natural Science Foundation of China (Grant Nos. 41601554, 41807495 & 51979197), Science and Technology Project of Wenzhou Science and Technology Bureau (Grant Nos. S20180005 & G20190026), and Science Research Funding of Wenzhou Medical University (Grant No. QTJ18032). We acknowledge the Environmental Stable Isotope Lab (Chinese Academy of Agricultural Sciences, Beijing, China) for their analytical support.

Supplementary data

Supplementary data to this article can be found online at https://doi.org/10.1016/j.scitotenv.2020.137975.

References

Adebowale, T., Surapaneni, A., Faulkner, D., McCance, W., Wang, S., Currell, M., 2019. Delineation of contaminant sources and denitrification using isotopes of nitrate near a wastewater treatment plant in peri-urban settings. Sci. Total Environ. 651, 2701–2711.

Aravena, R., Robertson, W.D., 1998. Use of multiple isotope tracers to evaluate denitrification in ground water: study of nitrate from a large-flux septic system plume. Ground Water 36, 975–982.

Biddau, R., Cidu, R., Da Pelo, S., Carletti, A., Ghiglieri, G., Pittalis, D., 2019. Source and fate of nitrate in contaminated groundwater systems: assessing spatial and temporal variations by hydrogeochemistry and multiple stable isotope tools. Sci. Total Environ. 647, 1121–1136.

Burow, K.R., Nolan, B.T., Rupert, M.G., Dubrovsky, N.M., 2010. Nitrate in groundwater of the United States, 1991–2003. Environ. Sci. Technol. 44, 4988–4997.

Carey, R.O., Migliaccio, K.W., Brown, M.T., 2011. Nutrient discharges to Biscayne Bay, Florida: trends, loads, and a pollutant index. Sci. Total Environ. 409, 530–539.

Chen, D.J., Shen, H., Hu, M.P., Wang, J.H., Zhang, Y.F., Dahlgren, R.A., 2018. Legacy nutrient dynamics at the watershed scale: principles, modeling, and implications. Adv. Agron. 149, 237–313.

Ding, J., Xi, B., Gao, R., He, L., Liu, H., Dai, X., Yu, Y., 2014. Identifying diffused nitrate sources in a stream in an agricultural field using a dual isotopic approach. Sci. Total Environ. 484, 10–18.

Dong, X., Mei, K., Shang, X., Huang, S.H., Huang, H., 2016. Analysis of variation trend of water quality based on Mann–Kendall test and rescaled range analysis. J. Ecol. Rural Environ. 32, 277–282 (in Chinese).

Flipse, W.J., Bonner, F.T., 1985. Nitrogen-isotope ratios of nitrate in ground-water under fertilized fields, Long Island, New York. Ground Water 23, 59–67.

Granger, J., Sigman, D.M., Lehmann, M.F., Tortell, P.D., 2008. Nitrogen and oxygen isotope fractionation during dissimilatory nitrate reduction by denitrifying bacteria. Limnol. Oceanogr. 53, 2533–2545.

Haas, M.B., Guse, B., Fohrer, N., 2017. Assessing the impacts of best management practices on nitrate pollution in an agricultural dominated lowland catchment considering environmental protection versus economic development. J. Environ. Manag. 196, 347–364.

Hord, N.G., 2011. Dietary nitrates, nitrites, and cardiovascular disease. Curr. Atheroscler. Rep. 13, 484–492.

Hu, M., Liu, Y., Zhang, Y., Dahlgren, R.A., Chen, D., 2019a. Coupling stable isotopes and water chemistry to assess the role of hydrological and biogeochemical processes on riverine nitrogen sources. Water Res. 150, 418–430.

Huang, H., Wang, Z., Xia, F., Shang, X., Liu, Y., Zhang, M., Dahlgren, R.A., Mei, K., 2017. Water quality trend and change-point analyses using integration of locally weighted polynomial regression and segmented regression. Environ. Sci. Pollut. Res. 24, 15827–15837.

Hu, M., Wang, Y., Du, P., Shui, Y., Cai, A., Lv, C., Bao, Y., Li, Y., Li, S., Zhang, P., 2019b. Tracing the sources of nitrate in the rivers and lakes of the southern areas of the Tibetan Plateau using dual nitrate isotopes. Sci. Total Environ. 658, 132–140.

Huang, H., Wang, Z., Chen, D., Xia, F., Shang, X., Liu, Y., Dahlgren, R.A., Mei, K., 2018. Influence of land use on the persistence effect of riverine phosphorus. Hydrol. Process. 32, 118–125.

Ji, X., Xie, R., Hao, Y., Lu, J., 2017. Quantitative identification of nitrate pollution sources and uncertainty analysis based on dual isotope approach in an agricultural watershed. Environ. Pollut. 229, 586–594.

Kendall, C., 1998. Tracing sources and cycling of nitrate in catchments. In: Kendall, C., McDonnell, J.J. (Eds.), Isotope Tracers in Catchment Hydrology. Elsevier, Amsterdam, pp. 519–576.

Kendall, C., McDonnell, J.J., 1998. Isotope Tracers in Catchment Hydrology. Elsevier, Amsterdam.

Kendall, C., Elliott, E.M., Wankel, S.D., 2007. Tracing anthropogenic inputs of nitrogen to ecosystems. Stable Isotopes in Ecology and Environmental Science, 2nd ed Blackwell Publishing Ltd, pp. 375–449.

Li, S.L., Liu, C.Q., Li, J., Liu, X.L., Chetelat, B., Wang, B.L., Wang, F.S., 2010. Assessment of the sources of nitrate in the Changjiang River, China using a nitrogen and oxygen isotopic approach. Environ. Sci. Technol. 44, 1573–1578.

Li, X.Y., Ding, Y.J., Han, T.D., Xu, J.Z., Kang, S.C., Wu, Q.B., Sillanpää, M., Yu, Z.B., Yu, C.R., 2017. Seasonal variations of organic carbon and nitrogen in the upper basins of Yangtze and Yellow Rivers. J. Mt. Sci. 14, 1577–1590.

Li, C., Li, S.L., Yue, F.J., Liu, J., Zhong, J., Yan, Z.F., Zhang, R.C., Wang, Z.J., Xu, S., 2019. Identification of sources and transformations of nitrate in the Xijiang River using nitrate isotopes and Bayesian model. Sci. Total Environ. 646, 801–810.

Liao, Z.L., 2015. Study on the Contamination of Atmospheric Nitrogen Deposition in Wenzhou Region. Wenzhou Medical University, Wenzhou, Zhejiang, China (in Chinese).

Liu, C.Q., Li, S.L., Lang, Y.C., Xiao, H.Y., 2006. Using $\delta^{15}N$- and $\delta^{18}O$-values to identify nitrate sources in karst ground water, Guiyang, Southwest China. Environ. Sci. Technol. 40, 6928–6933.

Liu, T., Wang, F., Michalski, G., Xia, X., Liu, S., 2013. Using ^{15}N, ^{17}O, and ^{18}O to determine nitrate sources in the Yellow River, China. Environ. Sci. Technol. 47, 13412–13421.

Lu, L., Cheng, H., Pu, X., Liu, X., Cheng, Q., 2015. Nitrate behaviors and source apportionment in an aquatic system from a watershed with intensive agricultural activities. Environ. Sci.: Process. Impacts 17, 131–144.

Mariotti, A., Germon, J.C., Hubert, P., Kaiser, P., Letolle, R., Tardieux, A., Tardieux, P., 1981. Experimental-determination of nitrogen kinetic isotope fractionation — some principles — illustration for the denitrification and nitrification processes. Plant Soil 62, 413–430.

Mayer, B., Bollwerk, S.M., Mansfeldt, T., Hutter, B., Veizer, J., 2001. The oxygen isotope composition of nitrate generated by nitrification in acid forest floors. Geochim. Cosmochim. Acta 65, 2743–2756.

Miller, M.P., Tesoriero, A.J., Capel, P.D., Pellerin, B.A., Hyer, K.E., Burns, D.A., 2016. Quantifying watershed-scale groundwater loading and in-stream fate of nitrate using high-frequency water quality data. Water Resour. Res. 52, 330–347.

National Research Council, 2001. Assessing the TMDL Approach to Water Quality Management. National Academy Press, Washington, DC.

Nestler, A., Berglund, M., Accoe, F., Duta, S., Xue, D., Boeckx, P., Taylor, P., 2011. Isotopes for improved management of nitrate pollution in aqueous resources: review of surface water field studies. Environ. Sci. Pollut. Res. 18, 519–533.

Parnell, A.C., Inger, R., Bearhop, S., Jackson, A.L., 2010. Source portioning using stable isotopes: coping with too much variation. PLoS One 5, e9672.

Rivett, M.O., Buss, S.R., Morgan, P., Smith, J.W.N., Bemment, C.D., 2008. Nitrate attenuation in groundwater: a review of biogeochemical controlling processes. Water Res. 42, 4215–4232.

Sarkkola, S., Koivusalo, H., Laurén, A., Kortelainen, P., Mattsson, T., Palviainen, M., Piirainen, S., Starr, M., Finér, L., 2009. Trends in hydrometeorological conditions and stream water organic carbon in boreal forested catchments. Sci. Total Environ. 408, 92–101.

Schilling, K., Zhang, Y.K., 2004. Baseflow contribution to nitrate-nitrogen export from a large, agricultural watershed, USA. J. Hydrol. 295, 305–316.
Sebestyen, S.D., Ross, D.S., Shanley, J.B., Elliott, E.M., Kendall, C., Campbell, J.L., Dail, D.B., Fernandez, I.J., Goodale, C.L., Lawrence, G.B., Lovett, G.M., McHale, P.J., Mitchell, M.J., Nelson, S.J., Shattuck, M.D., Wickman, T.R., Barnes, R.T., Bostic, J.T., Buda, A.R., Burns, D.A., Eshleman, K.N., Finlay, J.C., Nelson, D.M., Ohte, N., Pardo, L.H., Rose, L.A., Sabo, R.D., Schiff, S.L., Spoelstra, J., Williard, K.W.J., 2019. Unprocessed atmospheric nitrate in waters of the northern forest region in the US and Canada. Environ. Sci. Technol. 53, 3620–3633.
State Environment Protection Bureau of China, 2002. Environmental Quality Standards for Surface Water. China Environmental Science Press, Beijing (in Chinese).
von Toussaint, U., 2011. Bayesian inference in physics. Rev. Mod. Phys. 83, 943–999.
Wassenaar, L.I., 1995. Evaluation of the origin and fate of nitrate in the Abbotsford aquifer using the isotopes of ^{15}N and ^{18}O in NO_3^-. Appl. Geochem. 10, 391–405.
Wexler, S.K., Goodale, C.L., McGuire, K.J., Bailey, S.W., Groffman, P.M., 2014. Isotopic signals of summer denitrification in a northern hardwood forested catchment. Proc. Natl. Acad. Sci. 111, 16413–16418.
Widory, D., Kloppmann, W., Chery, L., Bonnin, J., Rochdi, H., Guinamant, J.L., 2004. Nitrate in groundwater: an isotopic multi-tracer approach. J. Contam. Hydrol. 72, 165–188.
World Health Organization, 2011. Guidelines for Drinking-Water Quality. 4th ed. (Geneva).
Xi, S., Liu, G., Zhou, C., Wu, L., Liu, R., 2015. Assessment of the sources of nitrate in the Chaohu Lake, China, using a nitrogen and oxygen isotopic approach. Environ. Earth Sci. 74, 1647–1655.
Xiao, L., Chen, Y.C., Cheng, J.B., 2011. Analysis of spatial-temporal distribution and its influencing factors of water quality in Shanxi headwater. Inner Mongolia Environmental Protection 23, 155–157 (in Chinese).
Xu, Z., Zhang, X., Yu, G., Sun, X., Wen, X., 2014. Review of dual stable isotope technique for nitrate source identification in surface- and groundwater in China. Environ. Sci. 35, 3230–3238 (Chinese).
Xue, D., Botte, J., De Baets, B., Accoe, F., Nestler, A., Taylor, P., Van Cleemput, O., Berglund, M., Boeckx, P., 2009. Present limitations and future prospects of stable isotope methods for nitrate source identification in surface- and groundwater. Water Res. 43, 1159–1170.
Xue, D., De Baets, B., Van Cleemput, O., Hennessy, C., Berglund, M., Boeckx, P., 2012. Use of a Bayesian isotope mixing model to estimate proportional contributions of multiple nitrate sources in surface water. Environ. Pollut. 161, 43–49.
Yang, L., Han, J., Xue, J., Zeng, L., Shi, J., Wu, L., Jiang, Y., 2013a. Nitrate source apportionment in a subtropical watershed using Bayesian model. Sci. Total Environ. 463, 340–347.
Yang, L., Mei, K., Liu, X., Wu, L., Zhang, M., Xu, J., Wang, F., 2013b. Spatial distribution and source apportionment of water pollution in different administrative zones of Wen-Rui-Tang (WRT) River watershed, China. Environ. Sci. Pollut. Res. 20, 5341–5352.
Yang, Y.Y., Toor, G.S., 2016. $\delta^{15}N$ and $\delta^{18}O$ reveal the sources of nitrate-nitrogen in urban residential stormwater runoff. Environ. Sci. Technol. 50, 2881–2889.
Yu, F., Shi, W.M., 2015. Nitrogen use efficiencies of major grain crops in China in recent 10 years. Acta Pedol. Sin. 52, 1311–1324 (in Chinese).
Zak, D., Kronvang, B., Carstensen, M.V., Hoffmann, C.C., Kjeldgaard, A., Larsen, S.E., Audet, J., Egemose, S., Jorgensen, C.A., Feuerbach, P., Gertz, F., Jensen, H.S., 2018. Nitrogen and phosphorus removal from agricultural runoff in integrated buffer zones. Environ. Sci. Technol. 52, 6508–6517.
Zhang, M., Zhi, Y., Shi, J., Wu, L., 2018. Apportionment and uncertainty analysis of nitrate sources based on the dual isotope approach and a Bayesian isotope mixing model at the watershed scale. Sci. Total Environ. 639, 1175–1187.